Unidirectional adaptive dynamics

Sudeshna Sinha
Theoretical Physics Group, Tata Institute of Fundamental Research, Homi Bhabha Road, Bombay 400 005, India
(Received 1 December 1993)

We have studied the temporal and spatial characteristics of a model of unidirectional adaptive dynamics on a chaotic lattice, introduced recently [Phys. Rev. Lett. **71**, 2010 (1993)]. Our analysis sheds light on the basic spatiotemporal structure and dynamical reasons underlying the many phases found in the model.

PACS number(s): 05.45.+b

I. INTRODUCTION

The dynamics of networks of chaotic elements is important not only as a model for complex nonlinear systems with many degrees of freedom, but also from the viewpoint of possible engineering applications [1]. Here we analyze in detail a model of unidirectional adaptive dynamics in a lattice of chaotic elements, proposed very recently by Sinha and Biswas [2]. The system is spatially extended, with local nonlinear dynamics along with a self-regulatory process incorporated as threshold dynamics. Such systems are relevant in the context of a variety of physical and biological phenomena (and even in social sciences such as economics). The object of this study is to investigate *analytically* the wealth of spatiotemporal structures this model yields, and characterize its "phases" and pattern dynamics.

Model

We first recall the model. It is a *one-dimensional unidirectional* model where time is discrete, labeled by n, space is discrete, labeled by i, $i=1,N$, where N is system size, and the state variable $x_n(i)$ (which in physical systems could be quantities like energy or pressure) is continuous. Each individual site in the lattice evolves chaotically under a suitable nonlinear map $f(x)$. The local map $f(x)$ was chosen to be the logistic map, which has widespread relevance as a prototype of chaos. So $f(x)=1-ax^2$, $x\in[-1.0,1.0]$, with the nonlinearity parameter a chosen in the chaotic regime ($a=2.0$ in all numerical experiments in Ref. [2]). On this chaotic lattice a self-regulatory threshold dynamics is incorporated. The adaptive mechanism is triggered when a site in the lattice exceeds the critical value x_c ($-1.0<x_c<1.0$), i.e., when a certain site $x_n(i)>x_c$. The supercritical site then relaxes (or "topples") by transporting its excess $\delta x=(x_n(i)-x_c)$ to its neighbor as follows:

$$\begin{aligned} &x_n(i)\rightarrow x_c \ , \\ &x_n(i+1)\rightarrow x_n(i+1)+\delta x \ . \end{aligned} \tag{1}$$

This algorithm thus induces a unidirectional nonlinear transport down the array (by initiating a domino effect). The boundary is open so that the "excess" may be transported out of the system. Note that the adaptive ("toppling") mechanism in the model is locally conservative, whereas the intrinsic dynamics of the elements is dissipative.

The nonlinear threshold adaptive dynamics is reminiscent of the Bak-Tang-Wiesenfeld algorithm [3], or the "sandpile" model, which gives to self-organized criticality (SOC). This model is, however, significantly different, the most important difference being that the self-regulatory mechanism now occurs on a chaotic "substrate," i.e., there is an "intrinsic" or "internal" deterministic dynamics at each site. Further, the state variable analogous to the integer "height" variable z in the sandpile model is continuous here. All this accounts for enhanced complexity, and this system is thus capable of exhibiting a wider repertoire of dynamics. So, unlike one-dimensional (1D) SOC, the one-dimensional model here is not trivial and can give rise to many interesting features, including a host of dynamical phases.

The dynamics depends on the algorithm for autonomously updating each site and propagating threshold coupling between sites. Here these two evolutionary steps are carried out separately. The adaptive dynamics begins after each step in the site dynamics and continues until the system has reached a steady state where all sites are less than critical, i.e., all $x(i)\leq x_c$, and the system is stationary, after which the next step in the site dynamics takes place. So the time scales of the two dynamics, the intrinsic chaotic dynamics of each lattice site and the adaptive relaxation, are adiabatically separable. The relaxation mechanism is much faster than the chaotic evolution, and this enables the system to relax completely before the next chaotic iteration. The complete dynamical picture then is as follows: After every time step in the chaotic evolution, n, the system undergoes a self-regulatory relaxation leading to stable "undercritical" configurations $\{x_n(i)\}$, after which the next chaotic iteration of the lattice takes place, governed by the nonlinear evolution mapping: $x_{n+1}(i)=f(x_n(i))$. A random driving force can also be introduced in our model. Under this, the system is perturbed at some site j in the lattice: $x_n(j)\rightarrow x_n(j)+\sigma$, where σ is the strength of the perturbation and j is chosen at random. Likewise, the random

 ©1994 The American Physical Society

driving force, operative at times scales comparable to the chaotic dynamics, is much slower than the adaptive dynamics. This scenario is similar to the SOC algorithm, where the driving force (perturbation) is very dilute. Thus the system is allowed to relax completely before the next perturbation and time is usually measured in units of the perturbing force (for example, in units of grains of "sand" added in the sandpile model of SOC) and the configurations studied are the relaxed configurations after each perturbation step. This is quite different from the coupled-map-lattice (CML) dynamics [4], where the coupling is incorporated in the map evolution step.

The relevant parameters in the model are the critical x_c, the strength of perturbation σ, and the system size N. The simulations were done with random initial conditions for the $x(i)$, and all transients were allowed to die. The quantities of interest are the temporal evolution of (a) the individual sites $x_n(i)$, and (b) the "avalanches," which are defined as the total number of "active" sites, i.e., sites that have "toppled" during the adaptive relaxation, denoted by s. The spatial aspects of interest are the distribution of $x(i)$ and the presence of clustering and coherence in space as indicated by the cluster distribution at any point in time [5].

Numerical simulations showed the presence of the following "phases" in parameter space: The first phase is the fixed point region which occurs when $x_c < 0.5$. Here the system goes to a coherent state where all sites $x_n(i)=x_c$ for all times (after transience). This phenomenon is independent of the perturbation strength and system size. Further, all avalanches are equal to system size (that is, all sites move in order to relax). In this parameter regime, then, the adaptive mechanism suppresses the underlying chaos in the lattice and yields spatiotemporal regularity.

This algorithm, with $x_c < 0.5$, may then be used as a tool for "controlling" [6] an ensemble of chaotic elements, as it can very effectively force the system to a temporally invariant and spatially coherent state: $x_n(i)=x_c$, $i=1,\ldots,N$ for all n. Note that this spatiotemporal control is robust with respect to system size and perturbation strengths. Couched in the language of control theory, we can consider x_c to be the desired state of the system [6]. (The algorithm is effective as long as the desired state, or x_c, is less than 0.5.) The "error signal" is then determined by the difference between the existing state and the desired state. A positive error signal triggers off the self-regulatory feedback mechanism which drives the system to adaptively control its dynamics back to the desired state (when error is zero).

When $0.5 < x_c < 1.0$, the dynamics of each individual site is attracted to a *cycle* whose periodicity depends on x_c. For example, by tuning x_c one obtains the following dynamical phases: for $0.5 < x_c \leq 0.809\ldots$, we get distinct 2 cycles in the temporal evolution of the avalanches and individual sites, for $x_c=0.84$ we have a 4 cycle, for $x_c=0.86$ a 6-cycle, for $x_c=0.88$ a 7 cycle, for $x_c=0.9$ a 10 cycle, and for $x_c=0.98$ a 4 cycle again. Now we proceed to obtain, as far as possible, a detailed analytical picture of the above dynamical phases.

II. ANALYSIS OF A SINGLE ELEMENT

The behavior of a single element x (the case of $N=1$) as a function of time n is very instructive as it sheds light on the basic structure of the dynamical phases in x_c space. (Note that there is *no* additional random driving force here, i.e., $\sigma=0$.) The first step in our analysis is to study the curves of the various iterates of the map. Let $f_n(x_c)$ denote the curve in x_c space of the nth iterate of the map with initial condition $x=x_c$. That is, (i) $n=0$, $f_0(x_c)=x_c$; (ii) $n=1$, $f_1(x_c)=1-2x_c^2$; (iii) $n=2$, $f_2(x_c)=1-2(1-2x_c^2)^2=-1-8x_c^4+8x_c^2$, and so on. In general,

$$f_n(x_c)=f\circ f_{n-1}(x_c)=f\circ f\circ\cdots\circ f(x_c)\ .$$

Figure 1 gives some of these curves. The important thing is the intersection of the f_n curves with f_0, i.e., the 45° line. Whenever the f_n curve crosses above the f_0 line we

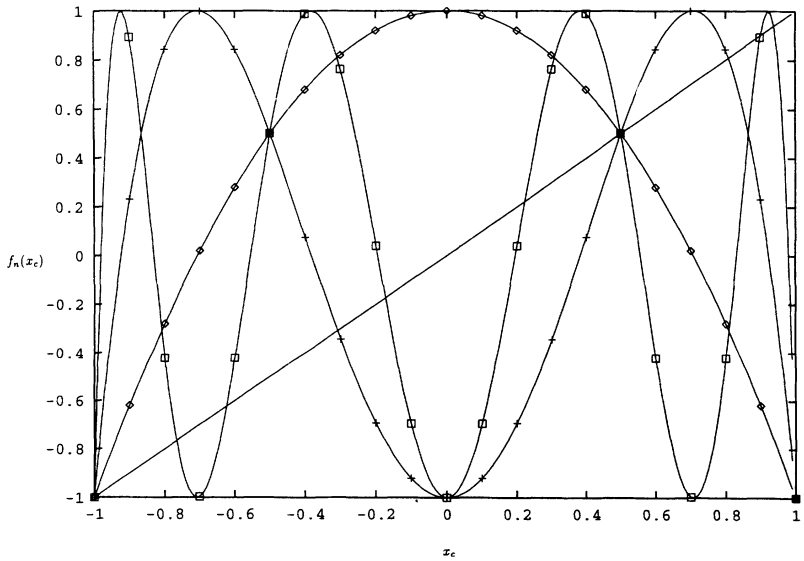

FIG. 1. Plot of $f_n(x_c)$ vs x_c, for $n=0,1,2,3$, where $f_n(x_c)$ is the nth iterate starting from initial condition $x=x_c$ of the logistic map: $f_0(x_c)$ (——), $f_1(x_c)$ (◇), $f_2(x_c)$ (+), $f_3(x_c)$ (□).

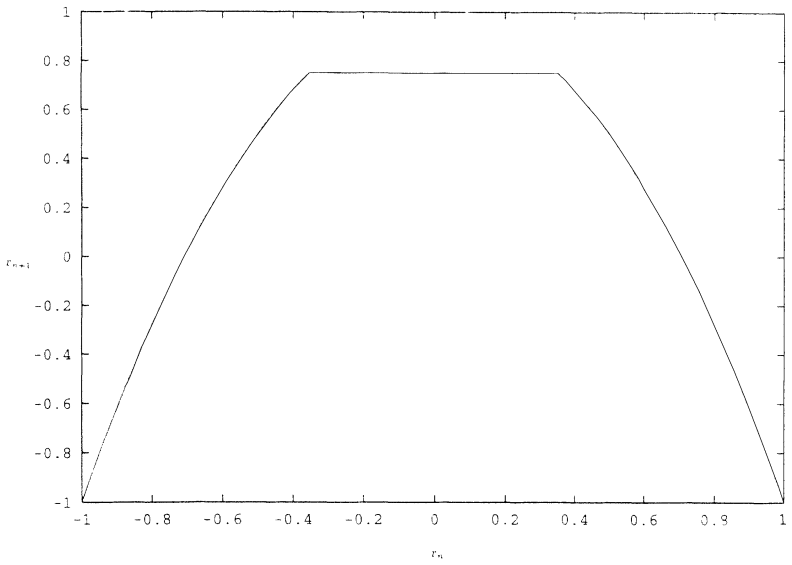

FIG. 2. The x_{n+1} vs x_n map for the dynamics of the unidirectional adaptive model, for a single element ($x_c=0.75$).

have an n cycle, as this implies that the nth iterate exceeds the critical value x_c and therefore is adapted back to x_c ($=f_0$, which is the first point of the cycle). Thus the threshold mechanism forces a regular "cyclic" evolution, whose period depends on x_c varying, for which we then get periods of all orders. *So the completely chaotic single element can now yield a wide variety of dynamical behavior determined by the critical x_c.* Further, it is instructive to construct a map corresponding to the dynamics of a single element for any arbitrary initial condition, at each chaotic update. Figure 2 gives such a local map. Note that the map is essentially the parabolic curve x_{n+1} vs x_n at $a=2.0$, cut off by the $x_{n+1}=x_c$ line.

A. Cycles

The first phase is the fixed-point region that occurs when f_1 lies above the f_0 curve. Clearly, this happens for values of x_c: $-1\le x_c\le 0.5$. Here we have a single point attractor: $x^*=x_c$. The second phase is the 2 cycle. This occurs when f_2 lies above the f_0, i.e., for $0.5<x_c<0.809\ldots$. Next we have a 4 cycle when the f_4 curve crosses above the f_0 line. This happens when $0.809\ldots<x_c<0.85\ldots$. Thus we can find the order of the cycle at any value of x_c by simply finding the smallest k that satisfies the equation $f_k(x_c)>x_c$. Likewise, the end points of the "windows" of parameter x_c, supporting a cycle of order k, are determined by the values of x_c that satisfy the equation $f_k(x_c)=x_c$.

B. "Stars"

Now $x_c=\frac{1}{2}$ is a fixed point of the map $f_1(x_c)=1-2x_c^2$. So if an iterate is equal to $\frac{1}{2}$, all the subsequent iterates must necessarily be $\frac{1}{2}$. When the initial point is $x_c=\frac{1}{2}$ the first iterate itself goes to the fixed point. There exist other values of x_c though, for which the map takes s ($s>1$) iterates to reach the fixed point. For these values of x_c, which we shall denote by x_s^* ($s=2,3,\ldots,\infty$), all curves $f_s, f_{s+1}, f_{s+2},\ldots,f_\infty$ will intersect at $\frac{1}{2}$. (Clearly, $x_1^*=\frac{1}{2}$.) This intersection of curves at points $(x_s^*,\frac{1}{2})$ on a plot of $f_n(x_c)$ ($n=1,2,\ldots,\infty$) vs x_c, has an intersecting "starlike" appearance, as evident from Fig. 3. These "stars" are interesting as around them we can have small parameter ranges of effectively chaotic behavior. This is because in the neighborhood of a star all the f_n,

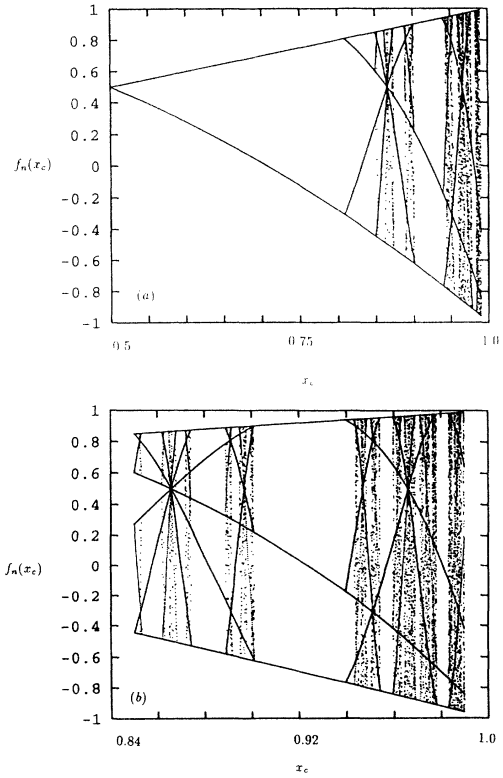

FIG. 3. Diagram of the curves $f_n(x_c)$ lying below $f_0(x_c)=x_c$, in the range (a) $x_c\in[0.5,1.0]$, and (b) $x_c\in[0.84,1.0]$. Note the "starlike" structures and windows.

$n=s, s+1, \ldots, \infty$ curves meet and then diverge, and so close to x_s^* we have many iterates below x_c, which implies that the order of the "cycle" around a star tends to be very large. It is also easy to see that the larger the value of x_c, the greater the number of iterates below x_c, and thus the dynamical behavior around higher order stars (i.e., stars with large s) approaches chaos more closely.

Clearly the location of the sth order stars on the x_c axis is given as a solution of the equation

$$f_s(x_c)=\tfrac{1}{2} . \tag{2}$$

A good way of formulating the solution to the above is to consider the inverse map:

$$f^{-1}(x)=\pm\sqrt{\tfrac{1}{2}(1-x)} \tag{3}$$

with the positive (right) branch denoted by $R(x)$ and the negative (left) branch by $L(x)$. The solution of Eq. (2) is then simply the inverse map composed s times:

$$x_s^*=f^{-1}\circ f^{-1}\circ\cdots\circ f^{-1}(\tfrac{1}{2}) . \tag{4}$$

Various solutions will be obtained, determined by whether $f^{-1}(x)$ is the left or right branch, and each solution is uniquely and completely represented by a sequence of R and L operators.

Now, we give some useful properties of the R and L nonlinear operators.

(i) $L=-R$, i.e., $L<R$.

(ii) For $x_1<x_2$, $R(x_1)>R(x_2)$ and $L(x_1)<L(x_2)$.

(iii) For $x<\frac{1}{2}$, $R(x)>\frac{1}{2}>x$ [and $L(x)<-\frac{1}{2}$], and vice versa.

(iv) When we compose f^{-1} with itself, there are four sequences possible: $L\circ L$, $L\circ R$, $R\circ L$, and $R\circ R$. Using the relations above, it is easy to see that these are ordered as

$$L\circ L<L\circ R<R\circ R<R\circ L .$$

Similarly, at the next stage we obtain the ordering:

$$L\circ L\circ L<L\circ L\circ R<L\circ R\circ R<L\circ R\circ L$$
$$<R\circ R\circ L<R\circ R\circ R<R\circ L\circ R<R\circ L\circ L .$$

One can continue this process and obtain an ordered set of the different sequences generated by the composition of any arbitrary number of inverse maps.

(v) The number of distinct sequences that can be generated by composing k maps $=2^k$. This arises simply from the fact that any position in the sequence of length k can take the value R or L (i.e., one of two values) independently.

Note two additional properties for the case of stars, which simplify their analysis:

(i) $R\circ R(\frac{1}{2})=R(\frac{1}{2})=\frac{1}{2}$, which implies $R^n(\frac{1}{2})=\frac{1}{2}$, i.e., $\frac{1}{2}$ is a fixed point of the right branch of the inverse map.

(ii) $L\circ R(\frac{1}{2})=L(\frac{1}{2})=-\frac{1}{2}$.

Now we would like to generate a sequence of stars that is guaranteed to be "visible (in Fig. 3), that is, we would like to eliminate the spurious roots of Eq. (2). A spurious root is one that has an iterate leading up to $\frac{1}{2}$ and has a value greater than itself (i.e., one of the iterates starting from x_s^* and going on to $\frac{1}{2}$ is $>x_s^*$). In the sequence that determines the value of x_s^*, the subsequences are the intermediate iterates. For example, for $x_4^*=R\circ R\circ L\circ L(\frac{1}{2})$, the intermediate iterates are $L(\frac{1}{2})$, $L\circ L(\frac{1}{2})$, and $R\circ L\circ L(\frac{1}{2})$. Clearly, $L\circ L(\frac{1}{2})<L(\frac{1}{2})<0<x_c$, but $R\circ L\circ L(\frac{1}{2})>x_c$. So this value of x_4^* is spurious and will not be visible in Fig. 3. In this fashion, we can then easily check to see which x_s^* are spurious.

It is easy to see that there exists one set of symbols that is always "visible" and also has many interesting properties. This is the sequence of x_s^* generated by $R\circ L^{s-1}$. Since all the iterates leading up to $\frac{1}{2}$ are negative here, they all lie below x_s^*. Further this set is ordered in s as follows: $x_s^*>x_{s-1}^*$. This is because $R\circ L^s>R\circ L^{s-1}$, as $L\circ L^{s-1}<L^{s-1}$ and $R(x_1)>R(x_2)$ when $x_1<x_2$.

We can then obtain a set of x_s^* values, corresponding to RL^{s-1}: For example, (i) $s=1$, $x_1^*=R(\frac{1}{2})=0.5$; (ii) $s=2$, $x_2^*=R\circ L(\frac{1}{2})=0.866\ldots$; (iii) $s=3$, $x_3^*=R\circ L\circ L(\frac{1}{2})=0.966\ldots$; (iv) $s=4$, $x_4^*=R\circ L\circ L\circ L(\frac{1}{2})=0.991\ldots$, and so on. A plot of the logarithm (to base 2) of $(1-x_s^*)$ vs s clearly is a straight line (see Fig. 4), with slope equal to -2. That is,

$$1-x_s^*\sim 4^{-s} , \tag{5}$$

which implies

$$\lim_{s\to\infty}\frac{x_{s+2}^*-x_{s+1}^*}{x_{s+1}^*-x_s^*}=\frac{1}{4} . \tag{6}$$

This can be obtained from analytical considerations as follows. First, we would like to get a map connecting x_s^* to x_{s+1}^*. Since, $L=-R$, we have

$$x_s^*=R\circ L^{s-1}(\tfrac{1}{2})=R\circ(-R)\circ L^{s-2}(\tfrac{1}{2})=R(-x_{s-1}^*) ,$$

which yields the general recursion relation

$$x_s^*=\sqrt{\tfrac{1}{2}(1+x_{s-1}^*)} . \tag{7}$$

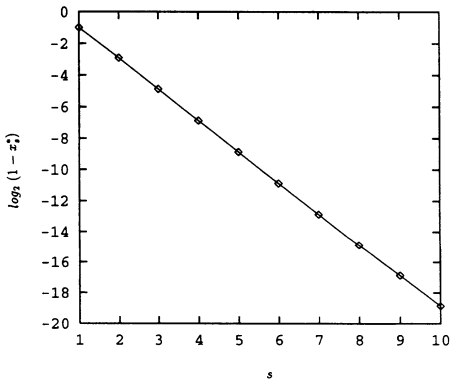

FIG. 4. Plot of $\log_2(1-x_s^*)$ vs s, where x_s^* is the sth order star given by $RL^{s-1}(\frac{1}{2})$.

For example, for $s=2$, $x_2^*=\sqrt{\frac{1}{2}(1+x_1^*)}=\sqrt{3}/2=0.866\ldots$, and for $s=3$, $x_3^*=\sqrt{\frac{1}{2}(1+x_2^*)}=\sqrt{(2+\sqrt{3})/4}=0.966\ldots$, and so on. Now the slope of the map x_s^* vs x_{s-1}^* [given by Eq. (7)] is equal to

$$\frac{1}{4}\frac{1}{\sqrt{\frac{1}{2}(1+x_{s-1}^*)}}\ .$$

At values close to 1, the slope is then close to $\frac{1}{4}$. Thus Eq. (6) follows.

C. Windows

In the x_c parameter space, we can find "windows" of various cycles. These are intervals on x_c where the following equation is satisfied:

$$\begin{aligned} &T(x_c)=k \quad \text{iff}\ , \\ &f_k(x_c)\geq x_c\ , \\ &f_{k'}(x_c)<x_c \quad \text{for all } k'<k\ . \end{aligned} \tag{8}$$

Period $T(x_c)$ is a piecewise continuous function of x_c. Now for every cycle of order k there will be many windows (see Fig. 5). The number of windows is determined by the number of times the $f_k(x_c)$ curves touch 1.0. It is evident from Fig. 1 that this is equal to 2^{k-1} in the interval $[-1,1]$. If we consider the positive half of the interval, as we shall do henceforth (as this is the relevant section of x_c), the number of windows of order k is 2^{k-2} (as the f_k curves are symmetric about 0). (Further, between every k window there are two $k+1$ windows—see Fig. 5. This is again expected from inspection of f_k and f_{k+1} curves in Fig. 1.)

We can label the windows by index n, where the window closest to 1.0 is $n=1$, and so on, up to $n=2^{k-2}$. Let the location of the midpoint of the nth window be denoted by $x_w^k(n)$ [7]. As in the case of stars, a good way of formulating $x_w^k(n)$ is to consider the inverse map given by Eq. (3), with the positive (right) branch denoted by $R(x)$ and the negative (left) branch by $L(x)$. The midpoint of a window of order k (for k large, when windows are narrow) is given by the condition $f_k(x_c)=1.0$, which implies the condition $f_{k-1}(x_c)=0$. Then the inverse map composed $k-1$ times determines x_w^k:

$$f^{-1}\circ f^{-1}\circ\cdots\circ f^{-1}(0)=x_w^k\ .$$

Now the different combinations of the letters R and L in the composed inverse mapping determine the different windows. As mentioned before, clearly there are 2^{k-1} distinct sequences that can be generated from the two letters R and L in a sequence of length $k-1$. That is, there are 2^{k-1} windows. This is exactly the number deduced from examination of the $f_k(x_c)$ curves in Fig. 1. (When we are considering only positive x_w^k we have half the number $=2^{k-2}$, as half the total number of sequences begin with L and thus are negative.)

Now $x_w^k(n)$, has interesting properties, for large k, where $x_w^k(n)\to 1.0$ (note that 1.0 is the only positive limit point, or "accumulation point," of the windows; see analysis below). Figure 6 shows $[1-x_w^k(n)]$ vs n, for a series of windows $n=1,2,\ldots,10$ for cycles of the order $k=6$, 7, and 8. When plotted on a log-log scale (base 2) the curves for different k are clearly parallel to each other, with the difference between the curves equal to 2. Further, for large n, the curves are quite straight, with slope approximately equal to 2.

So heuristically, by examination of Fig. 6 we can write down the relation

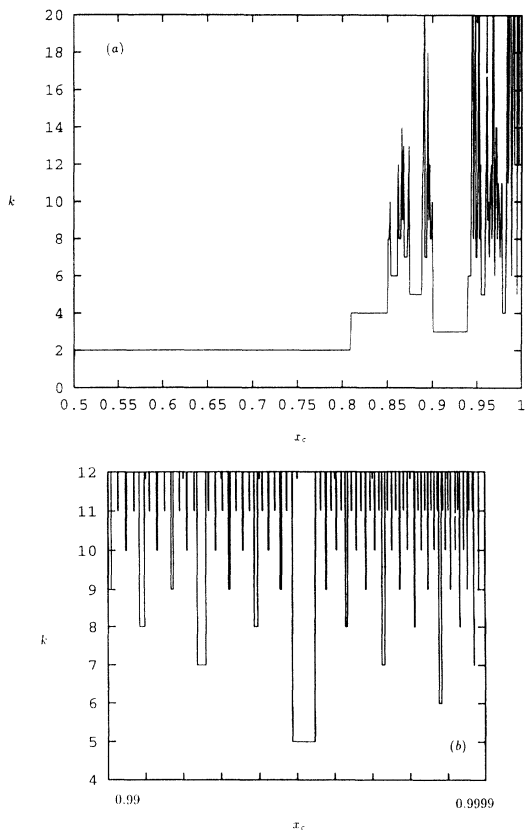

FIG. 5. Order k of the cycle vs x_c, for (a) $x_c\in[0.5,1.0]$ with k going up to 20 and (b) $x_c\in[0.99,0.9999]$ with k going up to 12.

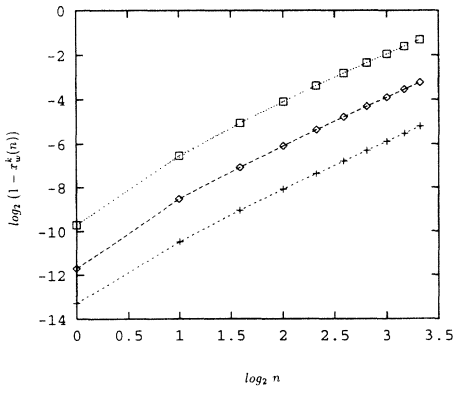

FIG. 6. Plot of $\log_2[1-x_w^k(n)]$ vs $\log_2 n$, where $x_w^k(n)$ is the value of x_c for the nth window supporting a cycle of period k, for $k=6$ (□), 7 (◇), and 8 (+).

$$[1-x_w^k(n)]=c_k n^{-\delta_k^n} , \tag{9}$$

where $c_k/c_{k+1}=4$ and δ_k^n is independent of k and also saturates to a value close to 2, as n grows larger (i.e., the curves tend towards straight lines on a log-log plot for large n).

The observation $c_k/c_{k+1}=4$ can be obtained from analytical considerations as follows: First we would like to get a map connecting $x_w^k(n)$ to $x_w^{k+1}(n)$. Now, if we consider a set of N_w windows $x_w^k(n)$, $n=1,2,\ldots,N_w$, such that all $x_w^k(n)$ are close to 1.0, it is easy to see that these are generated by composing R with the smallest windows at the preceding order $k-1$ [using property (ii) of Sec. II B]. Note that the smallest windows are equal to the negative of the largest windows; i.e., $-x_w^{k-1}(n)$, $n=1,2,\ldots,N_w$ [in terms of symbols, it implies that $x_w^k(n)$ is obtained by replacing the first R symbols of $x_w^{k-1}(n)$ by L, and then adding R to the left]. So the general recursion relation for the windows is

$$x_w^k(n)=\sqrt{\tfrac{1}{2}[1+x_w^{k-1}(n)]} . \tag{10}$$

For example, the first window of order k, i.e., with $n=1$ and closest to 1.0, is the combination giving rise to the largest value of x_c, and this is the sequence $R\circ L^{k-2}(0)$. Explicitly, then the first few cases of k are the following:

(i) For $k=2$, $R(0)$ gives $x_w^2(1)=1/\sqrt{2}$.

(ii) For $k=3$, $R\circ L(0)$ gives $x_w^3(1)=\sqrt{\frac{1}{2}[1+x_w^2(1)]}=\sqrt{\frac{1}{2}(1+1/\sqrt{2})}$.

(iii) For $k=4$, $R\circ L\circ L(0)$ gives

$$x_w^4(1)=\sqrt{\tfrac{1}{2}[1+x_w^3(1)]}=\{\tfrac{1}{2}[1+\sqrt{\tfrac{1}{2}(1+1/\sqrt{2})}]\}^{1/2} .$$

The limiting case for the first window is obtained as follows:

$$[\tfrac{1}{2}+\tfrac{1}{2}(\tfrac{1}{2}+\tfrac{1}{2}\sqrt{\tfrac{1}{2}+\cdots})^{1/2}]^{1/2}=x_w^k(1) ,$$

which in the large k limit implies

$$\sqrt{\tfrac{1}{2}[1+x_w^k(1)]}=x_w^k(1) , \tag{11}$$

which gives (taking the positive solution) $x_w^k(1)\to 1$ as $k\to\infty$.

Now the slope of the map $x_w^k(n)$ vs $x_w^{k-1}(n)$ is equal to

$$\frac{1}{4}\frac{1}{\sqrt{\frac{1}{2}[1+x_w^{k-1}(n)]}} .$$

At values close to 1, the slope is then close to $\frac{1}{4}$. It then follows that

$$\frac{x_w^{k+2}(n)-x_w^{k+1}(n)}{x_w^{k+1}(n)-x_w^k(n)}=\frac{1}{4} . \tag{12}$$

This is exactly what is observed in numerical experiments.

Now we investigate the behavior of the exponent δ_k^n from the relation

$$\frac{1-x_w^k(n)}{1-x_w^k(n-1)}=\left[\frac{n}{n-1}\right]^{-\delta_k^n} . \tag{13}$$

Several δ_k^n's were generated using Eqs. (10) and (13). First, we find that for different values of k one obtains almost identical values of δ_k^n, which is as expected from the fact that the curves for different k are parallel in Fig. 6. Figure 7 shows the relation of δ_k^n with respect to n. It is clear that, as n increases, δ_k^n tends to saturate to a value ~ 2.1. That is, for large n we have reasonable scaling behavior, with an exponent that is independent of k and n.

Lastly, we would like to discuss the "visibility" of these windows, that is, focus on the elimination of spurious roots of Eq. (8). Some windows may be "swallowed" by lower order windows. That is, a window of order k, at $x_w^k(n)$, may fall inside a window of order k', where $k'<k$, in which case only the k' window will be observed. So, in order to be "visible" (in Fig. 3), by the argument used in Sec. II B, there should be no iterate leading up to 0 that has value greater than itself [i.e., all iterates starting from $x_w^k(n)$ and going on to 0 must be $<x_w^k(n)$]. In the sequence that determines the value of $x_w^k(n)$, the subsequences are the intermediate iterates. One can then easily check to see which windows are spurious. For example, for windows of order 7, generated by sequences, $f^{-1}\circ f^{-1}\circ f^{-1}\circ f^{-1}\circ f^{-1}\circ f^{-1}(0)$, we have the following:

(i) $n=1$, $x_w^7(1)=R\circ L\circ L\circ L\circ L\circ L(0)=0.9997\ldots$ (window visible).

(ii) $n=2$, $x_w^7(2)=R\circ L\circ L\circ L\circ L\circ R(0)=0.9973\ldots$ (window visible).

(iii) $n=3$, $x_w^7(3)=R\circ L\circ L\circ L\circ R\circ R(0)=0.9925\ldots$ (window visible).

(iv) $n=4$, $x_w^7(4)=R\circ L\circ L\circ L\circ R\circ L(0)=0.9853\ldots$ (window visible).

(v) $n=5$, $x_w^7(5)=R\circ L\circ L\circ R\circ R\circ L(0)=0.9757\ldots$ (window visible).

(vi) $n=6$, $x_w^7(6)=R\circ L\circ L\circ R\circ R\circ R(0)=0.9638\ldots$ (window visible).

(vii) $n=7$, $x_w^7(7)=R\circ L\circ L\circ R\circ L\circ R(0)=0.9495\ldots$ (window visible).

(viii) $n=8$, $x_w^7(8)=R\circ L\circ L\circ R\circ L\circ L(0)=0.9330\ldots$ (window not visible).

Of course, it is easy to see that the first windows of all orders ($n=1$, k arbitrary) are always "visible" as they are generated by $R\circ L^{k-2}(0)$ and all the iterates leading up to 0 are negative.

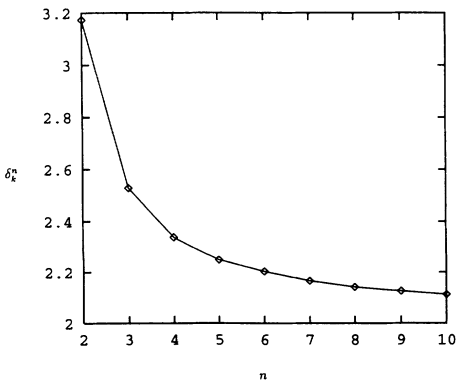

FIG. 7. Plot of the exponent δ_k^n [as determined by Eq. (13)] vs n.

III. SPATIAL ORGANIZATION

We would now like to focus on a generic lattice of size N, that is, focus on the asymptotic configurations $\mathbf{x}=\{x(1), x(2), \ldots, x(N)\}$ obtained from N elements evolving with the dynamics described by the map in Fig. 2, from random initial conditions. The important question here is the number of "states" possible when the single element executes a k cycle, k determined by x_c. (By "states" we mean distinct cycles in phase space, that is, distinct sets of k stable cyclic configurations, $\mathbf{x}_n^*$, $n=1, \ldots, k$.)

Note, that any configuration $\mathbf{x}$ the system does not return to, that is, anything that is not recurrent, is transient. We want to weed out all transients and look for the possible persisting asymptotic configurations $\mathbf{x}^*$. A fruitful way of looking at the problem is to realize that the dynamics of element $x(i)$ is affected only by elements $x(i')$ with $i'<i$, and not by elements with $i'>i$, as transport is unidirectional [8]. We elaborate the point further here: Note that the first element, $x(1)$, can be treated as an effective single element, as its dynamics is independent of the other elements, since none of the other elements $x(2)$, $x(3), \ldots, x(N)$ gives any "excess" to $x(1)$. Further, since each individual local map is chaotic, the iterates sample all regions of the interval $[-1,1]$ (i.e., is ergodic on the interval). So sooner or later $x(1)$ will exceed x_c and fall into a k cycle (k determined by x_c). Now, the second element is like the "edge" of the lattice for the first element. Thus $x(2)$ is influenced by $x(1)$ [as it can receive "excess" from it, in case $x(1)$ topples], but is not affected by the other elements $x(j)$, $j=3,4, \ldots, N$. Similarly, $x(3)$ is influenced by $x(1)$ and $x(2)$, but not by $x(j)$, $j=4,5, \ldots, N$, and is like the "edge" for the partial lattice $\{x(1),x(2)\}$. In general then, any element i is like an "edge" for the partial lattice, $\{x(1),x(2), \ldots, x(i-1)\}$, and the "excess" it receives is equivalent to the "drop rate" [5] of the partial lattice.

Now if the first element is executing a k order cycle: $x_1^*=x_c$, $x_2^*=f_1(x_c), \ldots, x_k^*=f_k(x_c)$, the excess it sends to its neighbor as a function of time is also a k order cycle: $\delta x,0,0, \ldots, 0$, where $\delta x=(f_{k+1}(x_c)-x_c)$. We have done a small numerical experiment: we study the evolution of a map $f(x)$, starting from random initial conditions, with the dynamics given by Fig. 2 [i.e., $f(x)=1-2x^2$, with the additional requirement: if $f(x)>x_c$ then $f(x)=x_c$]. Now we force this map with period k [where k is determined by x_c via Eq. (8)]. So, periodically the map gets "kicked" by an amount δx. Very soon we find that the map is synchronized with the driving frequency and is executing a k cycle itself. [Note that the usual logistic map, i.e., simply $f(x)=1-2x^2$, will not get synchronized to the driving frequency as our adaptively controlled map does, and in fact it most often goes out of the interval to be attracted to $-\infty$.]

Using this result we then have the following picture: The second element follows suit and gets into a k cycle, just as the first element. Now the two elements together will also eject excess from the edge as a k cycle. This forcing will drive the third element to a k cycle as well, and so on. So all the lattice elements will ultimately move as a k cycle. Of course, in general, none of the elements need to be in phase. In fact, their asymptotic configurations will depend very much on the initial random distribution of $x_0(i)$, $i=1, \ldots, N$. One can put an upper bound on the total number of different states possible. Since each site, after the first, can take k values independently, the number of states possible is k^{N-1}. So in order to estimate the total number of distinct states we have to consider all these configurations and see under what conditions they can recur. To illustrate the point we cite some specific examples below.

The case of the fixed point ($x_c \leq 1/2$) is trivial as discussed earlier. Only one state is possible here:

$$x_n(i)=x_1^*=x_c$$

for all sites i, at all times n. (This is also obtained from the fact that $k^{N-1}=1^{N-1}=1$, and so the maximum number of allowed states for fixed point dynamics in a lattice of any arbitrary size, is 1.) Let us now look at the simplest nontrivial case: two sites, with x_c in the two-cycle range ($0.5<x_c<0.809\ldots$). Here $N=2$ and $k=2$, and so $2^{2-1}=2$ possibilities must be considered. The first is the coherent one, where both elements are in phase executing the 2 cycle: x_c, x_2^*. So we have

$$\{x_c,x_c\} \rightarrow \{x_2^*,x_2^*\} \rightarrow \{x_c,x_c\} \ .$$

The second set of periodic configurations possible is

$$\{x_2^*,x_c\} \rightarrow \{x_c,x_2^*+\delta x\} \rightarrow \{x_2^*,x_c\} \ .$$

All other configurations can never recur, but will lead to one or the other of these two possible states. (For example, the transient configuration $\{x_c,x_2^*\}$ leads to $\{x_2^*,x_c\}$ in the next iteration, which leads to the out-of-phase cycle above.)

Now the out-of-phase cycle will not exist for all values of x_c. We can write down the condition for its existence analytically. It is simply the requirement:

$$f_1(x_2^*+\delta x) \geq x_c \ .$$

Figure 8(a) shows curves $f^{(1)}(x_c)=x_c$, $f^{(2)}(x_c)=x_2^*=1-2x_c^2$, and $f^{(3)}(x_c)=x_2^*+\delta x$, in the regions of x_c where they exist. Curves $f^{(1)}(x_c)$ and $f^{(2)}(x_c)$, which are the coherent state curves, exist in the entire interval $[0.5,0.809\ldots]$, whereas the out-of-phase curves, $f^{(1)}(x_c)$ and $f^{(3)}(x_c)$, exist only after $x_c \sim 0.67\ldots$ [when the condition $f_1(x_2+\delta x) \geq x_c$ is satisfied]. The curves obtained from simulations lie exactly on top of these. (The simulations are done by evolving around 500 random initial conditions and plotting the asymptotic values of the different elements in time.)

These curves indicate that for $x_c \in [0.5,0.67\ldots]$ we have only one state, namely, the coherent state where both elements are in phase and execute a 2 cycle, (x_c,x_2^*). For $x_c \in [0.67\ldots,0.809\ldots]$ we have two distinct states. The first is the coherent one and the second is the out-of-phase state where the first element executes the 2 cycle, (x_c,x_2^*), and the second element executes the two cycle, $(x_2^*+\delta x,x_c)$. Figure 8(b) shows a phase diagram obtained from the generic initial situation where (with no loss of generality) $x(1)=x_c$ and $x(2) \in [-1,1]$.

The figure gives the initial condition for $x(2)$ on the x axis, and x_c on the y axis. The regions marked with points yield the out-of-phase state, after transience, while the white regions yield the coherent state.

Next, we analyze two elements in the four-cycle regime ($0.809\ldots<x_c<0.85\ldots$), where the basic 4 cycle is $x_1^*=x_c,x_2^*,x_3^*,x_4^*$. We now have to consider $4^{2-1}=4$ possibilities.

(i) The first is $\{x_c,x_c\}$, which is the coherent state, giving the 4 cycle: $\{x_c,x_c\}\rightarrow\{x_2^*,x_2^*\}\rightarrow\{x_3^*,x_3^*\}\rightarrow\{x_4^*,x_4^*\}$.

(ii) Next we consider the initial condition, $\{x_c,x_4^*\}$. This gives rise to the following sequence:

$$\{x_2^*,x_c\}\rightarrow\{x_3^*,x_2^*\}\rightarrow\{x_4^*,x_3^*\}\rightarrow\{x_c,x_4^*+\delta x\}\rightarrow\{x_2^*,x_c\}\ .$$

The condition for this cycle to exist is $f_1(x_4^*+\delta x)\geq x_c$. (Note that $\{x_c,x_4^*\}$ is a transient as it can never recur.)

(iii) Next we consider the initial conditions, $\{x_c,x_3^*\}$. This gives rise to the following sequence:

$$\{x_2^*,x_4^*\}\rightarrow\{x_3^*,x_c\}\rightarrow\{x_4^*,x_2^*\}\rightarrow\{x_c,x_3^*+\delta x\}\rightarrow\{x_2^*,f_1(x_3^*+\delta x)\}\rightarrow\{x_3^*,x_c\}\ .$$

The condition for this cycle to exist is $f_2(x_3^*+\delta x)\geq x_c$. (Note that $\{x_c,x_3^*\}$ and $\{x_2^*,x_4^*\}$ are both transients as they can never recur.)

(iv) Lastly, we consider the initial condition, $\{x_c,x_2^*\}$. This gives rise to the following sequence:

$$\{x_2^*,x_3^*\}\rightarrow\{x_3^*,x_4^*\}\rightarrow\{x_4^*,x_c\}\rightarrow\{x_c,x_2^*+\delta x\}\rightarrow\{x_2^*,f_1(x_2^*+\delta x)\}\rightarrow\{x_3^*,f_2(x_2^*+\delta x)\}\rightarrow\{x_4^*,x_c\}\ .$$

The condition for this cycle to exist is $f_3(x_2^*+\delta x)\geq x_c$. (Note that $\{x_c^*,x_2^*\}$, $\{x_2^*,x_3^*\}$, and $\{x_3^*,x_4^*\}$ are all transients as they can never recur.)

Now the above conditions give various solution curves in x_c space, indicating the different values of $x(i)$, $i=1,2$, allowed in that region of x_c [see Fig. 9(a)]. We then have x_c, x_2^*, x_3^*, and x_4^* in the entire four-cycle window, $x_4^*+\delta x$ [from the fulfillment of condition (ii)] also in the entire window, $(x_3^*+\delta x)$ and $f_1(x_3^*+\delta x)$ [from the fulfillment of condition (iii)] after $x_c>0.837\ldots$, and lastly $(x_2^*+\delta x)$, $f_1(x_2^*+\delta x)$, and $f_2(x_2^*+\delta x)$ [from fulfillment of condition (iv)] after $x_c>0.8425\ldots$. These analytical curves are matched exactly by numerical simulations from several hundreds of random initial conditions.

These curves indicate that for $x_c\in[0.809\ldots, 0.838\ldots]$ we have two states. The first state is the coherent one where both elements are in phase and execute the 4 cycle, x_c, x_2^*, x_3^*, x_4^*. The second state is an out-of-phase one where the first element executes the 4 cycle, x_c, x_2^*, x_3^*, x_4^*; and the second element executes the 4 cycle, $x_4^*+\delta x$, x_c, x_2^*, x_3^*. For $x_c\in[0.838\ldots,0.8425\ldots]$, we have three distinct states. The first two are the ones given above, and the third is the out-of-phase state where the first element executes the 4 cycle, x_c, x_2^*, x_3^*, x_4^*; and the second element executes the 4 cycle, $x_3^*+\delta x$, $f_1(x_3^*+\delta x)$, x_c, x_2^*. For $x_c\in[0.8425\ldots,0.85\ldots]$, we have four distinct states. The first three are the ones given above; the fourth is the out-of-phase state where the first element executes the 4 cycle, x_c, x_2^*, x_3^*, x_4^*; and the second element executes the 4 cycle, $x_2^*+\delta x$, $f_1(x_2^*+\delta x)$, $f_2(x_2^*+\delta x)$, x_c. So, the maximum number of distinct cyclic states realized in this case is equal to 4 (in the parameter range, $0.84\ldots<x_c\sim0.85\ldots$), which is the number expected from the upper bound given by $4^{2-1}=4$. Figure 9(b)

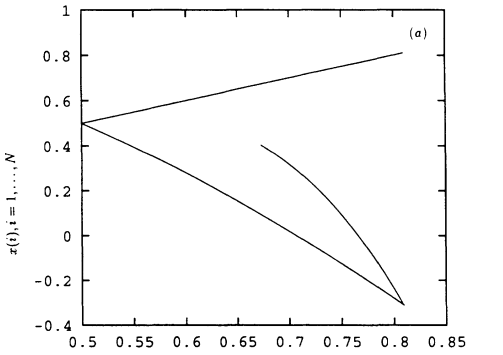

FIG. 8. (a) Plot of all the different values that the elements of a lattice, $x(i)$, $i=1,\ldots,N$, are allowed to take as they evolve in time (asymptotically) vs x_c. Here $N=2$, with x_c in the two-cycle regime ($0.5<x_c<0.809\ldots$). (b) Phase diagram obtained from the generic initial situation where $x(1)=x_c$ and $x(2)\in[-1,1]$. The x axis gives the initial condition for $x(2)$, and the y axis gives x_c. The regions marked with points yield the out-of-phase cycle, after transience, and the white regions yield coherent states.

shows a phase diagram obtained from the generic initial situation where (with no loss of generality) $x(1)=x_c$ and $x(2)\in[-1,1]$. The figure gives the initial condition for $x(2)$ on the x axis, and x_c on the y axis. The regions marked with the three different symbols yield the three different out-of-phase states while the white region yields the coherent state.

In order to examine the increase of complexity with increasing elements, we give one last example with three elements in the two-cycle regime ($0.5\ldots<x_c<0.809\ldots$). We now have to consider $2^{3-1}=4$ possibilities.

(i) The first is $\{x_c,x_c,x_c\}$, which is the coherent state, giving the 2 cycle, $\{x_c,x_c,x_c\}\rightarrow\{x_2^*,x_2^*,x_2^*\}$, where $x_2^*=1-2x_c^2$.

(ii) Next we consider the initial condition, $\{x_c,x_2^*,x_2^*\}$. This gives rise to the following sequence: $\{x_2^*,x_c,x_c\}\rightarrow\{x_c,x_2^*+\delta x,x_2^*\}\rightarrow\{x_2^*,x_c,x_c\}$. The condition for this cycle to exist is $f_1(x_2^*+\delta x)\geq x_c$. (Note that $\{x_c,x_2^*,x_2^*\}$ is a transient as it can never recur.)

(iii) Next we consider the initial condition, $\{x_c,x_2^*,x_c\}$. This gives rise to the following sequence: $\{x_2^*,x_c,x_2^*+\delta x\}\rightarrow\{x_c,x_2^*+\delta x,x_c\}\rightarrow\{x_2^*,x_c,x_2^*+\delta x_2\}\rightarrow\{x_c,x_2^*+\delta x,x_c\}$, where $\delta x_2=f_1(x_2^*+\delta x)-x_c$. The condition for this cycle to exist is condition (ii) plus the condition that $f_1(x_2^*+\delta x_2)\geq x_c$. (Note that $\{x_c,x_2^*,x_c\}$ and $\{x_2^*,x_c,x_2^*+\delta x\}$ are both transients as they can never recur.)

(iv) Lastly, we consider the initial condition, $\{x_c,x_c,x_2^*\}$. This gives rise to the following sequence: $\{x_2^*,x_2^*,x_c\}\rightarrow\{x_c,x_c,x_2^*+2\delta x\}\rightarrow\{x_2^*,x_2^*,x_c\}$. The condition for this cycle to exist is $f_1(x_2^*+2\delta x)\geq x_c$. (Note that $\{x_c,x_c,x_2^*\}$ is a transient as it can never recur.)

Now the above conditions give various solution curves in x_c space, indicating the allowed values of $x(i)$, $i=1,2,3$, in that region of x_c (see Fig. 10). We then have x_c and $1-2x_c^2$ in the entire two-cycle window (the coherent state), $x_2^*+\delta x$ [from the fulfillment of condition (ii)] after $x_c\sim 0.67\ldots$, $(x_2^*+\delta x_2)$ [from the simultaneous fulfillment of conditions (ii) and (iii)] after $x_c>0.67\ldots$, and lastly $(x_2^*+2\delta x)$ [from fulfillment of condition (iv)] after $x_c>0.75\ldots$ [9].

These curves indicate that for $x_c\in[0.5,0.67\ldots]$ we have only the coherent state where all the three elements are in phase executing the 2 cycle, (x_c,x_2^*). For $x_c\in[0.67\ldots,0.75\ldots]$ we have three cyclic states. The first is the coherent state given above. The second is an out-of-phase state where the first element executes the 2 cycle, (x_c,x_2^*); the second element executes the 2 cycle, $(x_2^*+\delta x,x_c)$; and the third element executes the 2 cycle, (x_2^*,x_c). The third state is another out-of-phase state where the first element executes the 2 cycle, (x_c,x_2^*); the second element executes the 2 cycle, $(x_2^*+\delta x,x_c)$; and the third element executes the 2 cycle, $(x_c,x_2^*+\delta x_2)$.

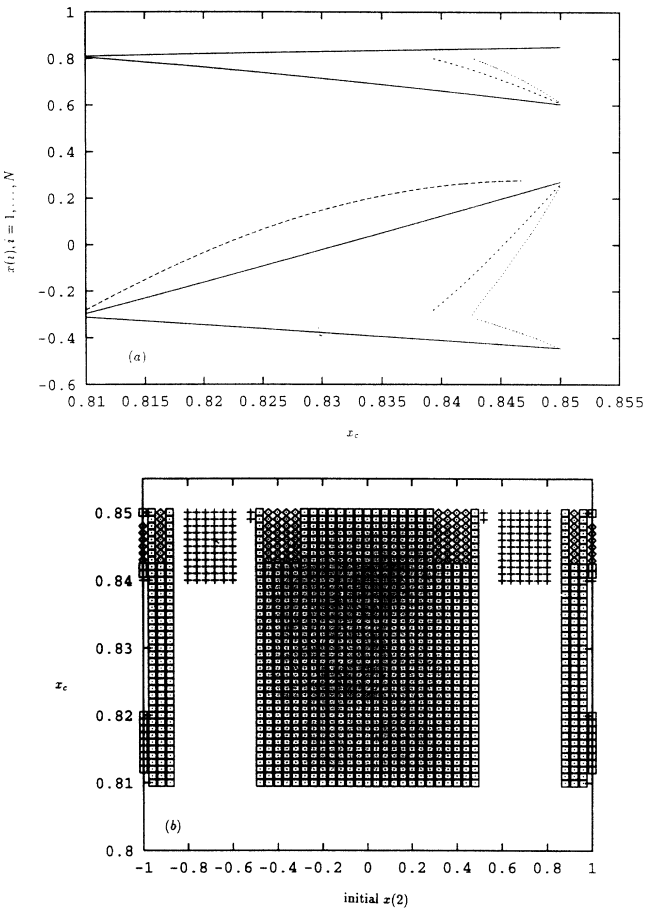

FIG. 9. (a) Plot of all the different values that the elements of a lattice, $x(i)$, $i=1,\ldots,N$ are allowed to take as they evolve in time (asymptotically) vs x_c. Here $N=2$, with x_c in the four-cycle regime ($0.809\ldots<x_c<0.85\ldots$). (b) Phase diagram obtained from the generic initial situation where $x(1)=x_c$ and $x(2)\in[-1,1]$. The x axis gives the initial condition for $x(2)$, and the y axis gives x_c. The regions marked with the symbols yield the three out-of-phase cyclic states, after transience [cyclic state 2 (□), cyclic state 3 (+), cyclic state 4 (◇)] and the white regions yield coherent states.

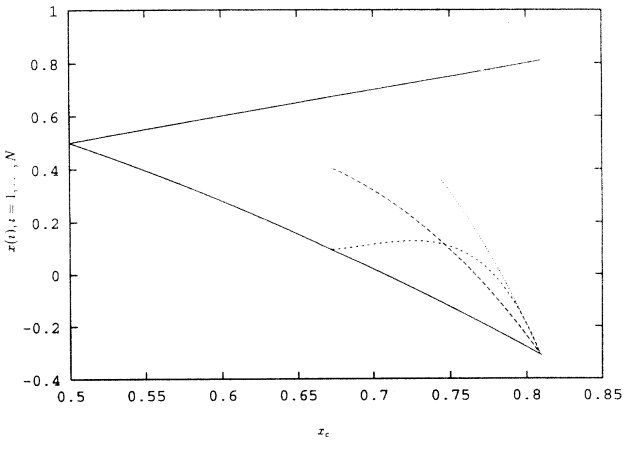

FIG. 10. Plot of all the different values that the elements of a lattice, $x(i)$, $i=1,\ldots,N$ are allowed to take as they evolve in time (asymptotically) vs x_c. Here $N=3$, with x_c in the two-cycle regime ($0.5<x_c<0.809\ldots$).

For $x_c \in [0.75\ldots, 0.809\ldots]$, we have four distinct states. The first three are the ones given above, and the fourth state is the out-of-phase state where the first element executes the 2 cycle, (x_c, x_2^*); the second element executes the 2 cycle, (x_c, x_2^*); and the third element executes the 2 cycle, $(x_2^* + 2\delta x, x_c)$. The maximum number of distinct cyclic states realized in this case (= 4, in the parameter range: $0.75\ldots < x_c \sim 0.809\ldots$) is again the number expected from the upper bound given by $2^{3-1}=4$.

In order to demonstrate the increasingly many distinct states possible as the lattice size and the order of the basic cycle of the individual elements increases, we plot in Fig. 11 the results of numerical simulations on a lattice with four elements in the four-cycle regime. The figure is obtained from examining the asymptotic states obtained from evolving 500 random initial conditions. On the x axis we have x_c and on the y axis we plot all the $x_n(i)$, $i=1,2,3,4$, over large n, for all initial conditions, after transience. The maximum number of distinct cycles obtained numerically (at $x_c \sim 0.85\ldots$) is 64, which again is the number expected from $k^{N-1}=4^{4-1}$. So a larger lattice, with larger k, has a lower chance of coherence, as the number of possible out-of-phase states grows enormously. Thus, it is clear that generically a lattice will not be homogeneous spatially. [Interestingly, a larger lattice has a good chance of developing a large cluster, in the direction of transport up to the open edge (see Fig. 12). This is because a cluster of size n_c, at some point in time, will exceed the critical value and eject $n_c\delta x$ to the element just adjacent to it. If n_c is reasonably large it is highly probable that this excess will make the neighboring site topple as well. So we have a "swallowing mechanism" by which the cluster can extend, and the bigger it is, the faster it grows towards the open edge.]

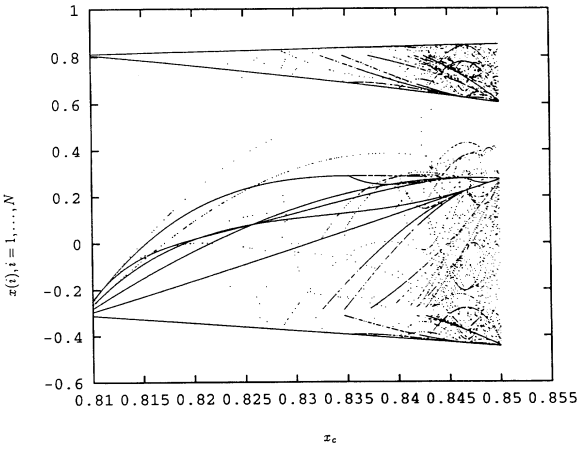

FIG. 11. Plot of all the different values the elements of a lattice take as they evolve in time (asymptotically), from 500 random initial conditions, for the case of $N=4$, with x_c in the four-cycle regime ($0.809\ldots < x_c < 0.85\ldots$).

IV. DISCUSSION

In summary, we have provided an analytical study of a model of unidirectional transport due to adaptive dynamics on a chaotic lattice, introduced recently (in Ref. [2]). Our study sheds light on the basic spatiotemporal structure and dynamical reasons underlying the many phases found in the model.

We would like to mention here some of the interesting extensions of this model that we have not yet treated analytically. The first is the effect of weak noise on the power spectrum of the unidirectional model. It was observed [2] that certain parameter ranges (x_c large), in the presence of noise, gave rise to $1/f^{\phi}$, $0<\phi\leq 1$ spectrum. The effect of finite σ was larger for the smaller lattices (as the ratio of the number of sites affected to total sites is larger here), while the larger ones were effectively regular. Note that in the cyclic window of order k the f_k curve touches 1.0 at around the middle of the window. All the subsequent curves $f_{k+1}, f_{k+2}, \ldots, f_\infty$ touch -1.0 at this value of x_c, as 1.0 leads to the unstable fixed point at -1.0 in its next iteration. So around x_c^k we have many diverging curves. In case of small perturbation then, the iterates can be pushed onto these curves, and will spend some time trapped in a "bottleneck" before it gets back to its k cycle. So the regular k periodic time

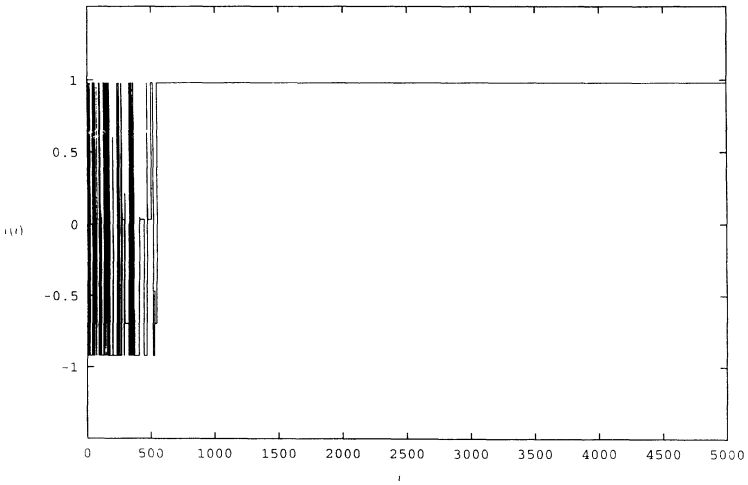

FIG. 12. Plot of $x(i)$ vs i, for a lattice of size $N=5000$, where $x(i)$ is the value of the state variable at site i, $i=1,2,\ldots,N$. Here $x_c=0.98$. Note the large cluster towards the edge [$x(j)=x_c=0.98$, $j\sim 600$ to 5000].

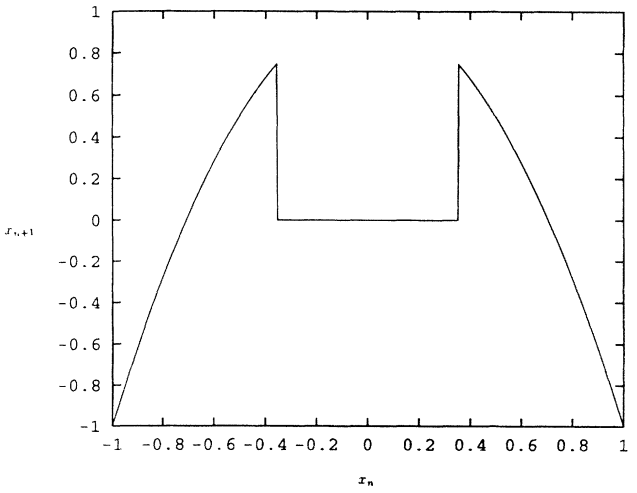

FIG. 13. x_{n+1} vs x_n map for the dynamics of the bidirectional adaptive model, with $x_0 \leq x_c$, for a single element ($x_c = 0.75$, $x_0 = 0.0$).

evolution is disrupted by bursts of irregularity. This results in $1/f^{\phi}$ spectrum, $0 < \phi \leq 1$, at the low frequency end, in addition to the peak at frequency $1/k$, as observed in numerical experiments.

Reference [2] also introduces the bidirectional model. This is given by the following modified relaxation algorithm: if $x_n(i) > x_c$, the supercritical site then relaxes to a value x_0, ($x_0 \leq x_c$) by transporting the excess $[x_n(i) - x_0]$ equally to its two neighbors:

$$\begin{aligned} &x_n(i) \rightarrow x_c \ , \\ &x_n(i+1) \rightarrow x_n(i+1) + \delta x \ , \\ &x_n(i-1) \rightarrow x_n(i-1) + \delta x \ , \end{aligned} \tag{14}$$

where $\delta x = (x_n(i) - x_c)/2$. This is more difficult to tackle analytically, as there is the dynamical possibility of a site, in the course of self-regulation, to "topple" many times as the disturbance moves back and forth in the lattice. Unlike the unidirectional model where the disturbance propagation is in one direction (so sites can topple just once), in the bidirectional case the disturbance spreads like "ripples" and can "refract." So we cannot use the argument of Sec. III, which allows us in the case of unidirectional transport to deduce that the individual elements of the lattice evolve cyclically (in fact they need not necessarily do so for all x_c in the bidirectional case). But the dynamics of a single element in the bidirectional model is still the same as that above, for $x_0 = x_c$, and so the basic structure of the dynamical phases is the same as in the unidirectional case. In fact, the temporal characteristics of the bidirectional model look like a "noisier" version of its unidirectional counterpart. Also, note that the case of $-1.0 \leq x_0 < x_c$ can be treated similarly, with the dynamics of a single element given by the map in Fig. 13, based on which the entire analysis of Sec. II can be carried through. Another interesting feature of bidirectional transport is that one obtains very distinct $1/f$ spectrum [2] here, for certain ranges of x_c, even when $\sigma = 0$, i.e., there is no additional noise. (Also the $1/f$ spectrum is more distinct for the bidirectional case as compared to its unidirectional counterpart, for it persists even at the lowest frequencies.)

In conclusion, the dynamics of this extended adaptive nonlinear system is amenable to extensive analytical study, and this contributes considerably to its interest and usefulness as a model for complex nonlinear phenomena.

ACKNOWLEDGMENTS

I would like to thank Deepak Dhar for several interesting ideas. Without his suggestions and directions a good part of the above analysis would not have been possible. It is also a pleasure to thank D. Sen, N. Deo, S. Jain, S. Ramaswamy, and R. Pandit for many stimulating questions and discussions.

[1] J. Crutchfield and K. Kaneko, in *Directions in Chaos*, edited by Hao Bai-Lin (World Scientific, Singapore, 1987), and references therein.

[2] S. Sinha and D. Biswas, Phys. Rev. Lett. **71**, 2010 (1993).

[3] P. Bak, C. Tang, and K. Weisenfeld, Phys. Rev. Lett. **59**, 381 (1987); Phys. Rev. A **38**, 364 (1988).

[4] R. Kapral, J. Math. Chem. **6**, 113 (1991), and references therein. This system further differs from the usual CML in having threshold as opposed to diffusive coupling. In this respect it is more like a biological system, e.g., the synapses of nerve tissue, or certain mechanical systems like chains of nonlinear springs, than a chemical system, e.g., a reaction diffusion equation.

[5] In certain contexts, some other quantities may be of interest, for instance, the dynamics and distribution of the "drop rate," i.e., the "excess" transported out of the system during relaxation, may be relevant.

[6] B. Huberman and E. Lumer, IEEE Trans. Circuits Syst. **37**, 547 (1990); S. Sinha, R. Ramaswamy, and J. Subba Rao, Physica D **43**, 118 (1990), and references therein.

[7] Windows become narrower with increasing k and n.

[8] Note that the direction of transport determined by Eq. (1) implies that the label i goes from 1 to N in the direction of transport, with element $x(N)$ being closest to the edge of the full lattice from where the total excess falls off.

[9] A rule of thumb to weed out transient configurations from asymptotic ones clearly is the following: In the direction of transport, an element with value x_c cannot be followed by one with value x_i, where x_i is a point on the k cycle. Rather, the following element must have value $x_i + n_c \delta x$, where n_c is the number of consecutive elements with value x_c just preceding it. (That is, a cluster of n_c sites at x_c, must be followed by a site at $x_i + n_c \delta x$.)